Catalytic Mechanism of Dichloromethane Dehalogenase from Methylophilus sp. Strain DM11 †

ARTICLE *in* BIOCHEMISTRY · OCTOBER 2003

Impact Factor: 3.02 · DOI: 10.1021/bi035016r · Source: PubMed

4 AUTHORS, INCLUDING:

Stéphane Vuilleumier
University of Strasbourg
112 PUBLICATIONS **2,828** CITATIONS

SEE PROFILE

Catalytic Mechanism of Dichloromethane Dehalogenase from *Methylophilus* sp. Strain DM11†

Nina V. Stourman,‡ James H. Rose,‡ Stephane Vuilleumier,§ and Richard N. Armstrong*,‡

Departments of Biochemistry and Chemistry and Center in Molecular Toxicology, Vanderbilt University School of Medicine, Nashville, Tennessee 37232-0146 USA, and Laboratoire de Microbiologie et de Genetique, FRE2326/CNRS, Universite Louis-Pasteur, F-67000 Strasbourg, France

Received June 13, 2003; Revised Manuscript Received July 17, 2003

ABSTRACT: The glutathione (GSH)-dependent dichloromethane dehalogenase from *Methylophilus* sp. strain DM11 catalyzes the dechlorination of CH_2Cl_2 to formaldehyde via a highly reactive, genotoxic intermediate, *S*-(chloromethyl)glutathione (GS-CH_2Cl). The catalytic mechanism of the enzyme toward a series of dihalomethane and monohaloethane substrates suggests that the initial addition of GSH to the alkylhalides is fast and that the rate-limiting step in turnover is the release of either the peptide product or formaldehyde. With the exception of CH_2ClF, which forms a relatively stable GS-CH_2F intermediate, the turnover numbers for a series of dihalomethanes fall in a very narrow range (1−3 s^{-1}). The pre-steady-state kinetics of the DM11-catalyzed addition of GSH to CH_3CH_2Br exhibits a burst of *S*-(ethyl)-glutathione ($k_b = 96 \pm 56$ s^{-1}) followed by a steady state with $k_{cat} = 0.13 \pm 0.01$ s^{-1}. The turnover numbers for CH_3CH_2Cl, CH_3-CH_2Br, and CH_3CH_2I are identical, indicating a common rate-limiting step. The turnover numbers of the enzyme with CH_3CH_2Br and CH_3CH_2I are dependent on viscosity and are very close to the measured off-rate of GSEt. The turnover number with CH_2I_2 is also dependent on viscosity, suggesting that a diffusive step is rate-limiting with dihaloalkanes as well. The rate constants for solvolysis of CH_3SCH_2Cl, a model for GS-CH_2Cl, range between 1 s^{-1} (1:1 dioxane/water) and 64 s^{-1} (1:10 dioxane/water). Solvolysis of the *S*-(halomethyl)glutathione intermediates may also occur in the active site of the enzyme preventing the release of the genotoxic species. Together, the results indicate that dissociation of the GS-CH_2X or GS-CH_2OH intermediates from the enzyme may be a relatively rare event.

A number of glutathione (GSH)[1] transferases are capable of catalyzing the dehalogenation of dichloromethane and related compounds to formaldehyde via the reactive *S*-(halomethyl)glutathione intermediate as illustrated in Scheme 1. In mammals, this reaction is principally catalyzed by the class theta GSH transferases and is thought to be responsible for the bioactivation of dihaloalkanes to mutagens (*1*−*8*). Some microorganisms use similar enzymes to initiate the acquisition of carbon or energy from dihalomethanes (*9*−*12*). The GSH-dependent dichloromethane dehalogenase from *Methylophilus* sp. strain DM11 is a very efficient catalyst in this regard. However, it is not clear how the bacteria mitigate the genotoxic effects of the heavy load of *S*-(halomethyl)glutathione produced during the catabolism of dihalomethanes.

It is established that both mammalian and bacterial enzymes, which catalyze the GSH-dependent dehalogenation of dihaloalkanes, also enhance the mutagenicity of the compounds in reversion assays with *Salmonella typhimurium*. The bacterial DM11 dehalogenase has a much higher catalytic efficiency (k_{cat}/K_M) toward dihalomethanes than do the mammalian class theta enzymes (*13*, *14*). Although a higher catalytic efficiency might be expected to lead to enhanced metabolic activation, the observed mutagenicity does not clearly correlate with catalytic efficiency (*13*, *14*). In fact, in one study the DM11 enzyme was found to be much less effective in the metabolic activation of CH_2Cl_2 than the rat GST T1−1 (*13*).

Scheme 1

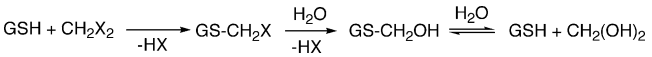

It is possible that the catalytic properties of the DM11 enzyme have evolved to minimize the formation of the presumed mutagen, free *S*-(halomethyl)glutathione. For example, GS-CH_2Cl is expected to be a very reactive species that may solvolyze to GS-CH_2OH while still bound in the active site of the enzyme, particularly if the product release steps are slow as illustrated in Scheme 2. Moreover, it is also possible that the enzyme may utilize a single molecule of GSH for multiple rounds of catalysis if the hydrolysis of GS-CH_2OH to formaldehyde on the enzyme surface is faster than peptide product release. The relatively low values of K_M^{CH2X2} and the fact that the turnover numbers for DM11-catalyzed reactions with many dihalomethanes fall in a very

† Supported by Grants R01 GM30910, P30 ES00267, T32 ES07028 from the National Institutes of Health.

* Address correspondence to this author. Email: r.armstrong@vanderbilt.edu. Fax: 615 343-2921. Tel: 615 343-2920.

‡ Vanderbilt University.

§ Universite Louis-Pasteur.

[1] Abbreviations: GSH, reduced glutathione; GSO_3^-, glutathione sulfonate; GSEt, *S*-(ethyl)glutathione; DTT, dithiothreitol; EDTA, ethylenediaminetetraacetic acid; IPTG, isopropylthioglucopyranoside; HEPES, 4-(2-hydroxyethyl)piperazine-1-ethanesulfonic acid; NAD, *β*-nicotinamide adenine dinucleotide; ACQ, 6-aminoquinoyl-*N*-hydroxysuccinimidylcarbamate.

10.1021/bi035016r CCC: $25.00
Published on Web 08/20/2003

Scheme 2

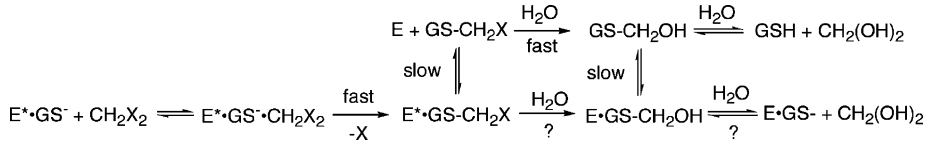

narrow range is consistent with a rate-limiting step in the reaction other than the initial halide displacement (*14*, *15*). However, the relative rates of the initial displacement reaction, solvolysis, and product release steps for these reactions are not known.

In this paper, the catalytic properties of the DM11 dehalogenase are probed with a series dihalomethane and monohaloethane substrates. The later compounds are substrate analogues that report on the initial halide displacement reaction without the complications of the subsequent chemistry that ensues with dihalomethane substrates. Rapid-quench kinetic results suggest that the initial displacement reaction is very fast relative to the turnover of the enzyme. The turnover numbers of the enzyme with CH_3CH_2Br and CH_3CH_2I are shown to be dependent on the viscosity of the reaction medium and are very close to the measured off-rate of GSEt. The turnover number of CH_2I_2 determined by iodide release is also dependent on viscosity, suggesting that a diffusive step, perhaps product release, is the rate-limiting step with dihaloalkanes as well. The rate constant for solvolysis of CH_3SCH_2Cl, a model for GS-CH_2Cl, was determined to range between 1 s^{-1} (1:1 dioxane/water) and 64 s^{-1} (1:10 dioxane/water). Taken together, the results indicate that release of the *S*-(halomethyl)glutathione intermediate from the enzyme may be a relatively rare event.

EXPERIMENTAL PROCEDURES

Materials. Competent cells of *Escherichia coli* BL21(DE3)*pLysS* were from Novagen (Madison, WI). Isopropyl-β-D-thiogalactopyrnoside (IPTG) and 1,4-dithiothreitol (DTT) were obtained from Research Organics (Cleveland, OH). Ampicillin, chloramphenicol, sodium acetate, triethylamine, EDTA (ethylenediaminetetraacetic acid), glycerol, sucrose, HEPES (4-(2-hydroxyethyl)piperazine-1-ethanesulfonic acid), glutathione, *S*-(ethyl)glutathione, NAD (β-nicotinamide adenine dinucleotide), and formaldehyde dehydrogenase from *Pseudomonas putida* were purchased from Sigma (St. Louis, MO). Dichloromethane, chlorobromomethane, dibromomethane, chloroiodomethane, diiodomethane, iodoethane, chloroethane, bromoethane, and 1,4-dioxane (anhydrous) were obtained from Aldrich (Milwaukee, WI) and used without further purification. Chloromethyl methyl sulfide (Aldrich) was purified by distillation. Chlorofluoromethane was obtained from Flura Corporation (Newport, TN). Water (HPLC grade) and anhydrous monobasic potassium phosphate were from Fisher Scientific (Pittsburgh, PA). Acetonitrile (HPLC grade) was from EM Science (Gibbstown, NJ). The fluorescence reagent AQC (6-aminoquinoyl-*N*-hydroxysuccinimidyl carbamate) was purchased from Waters (Milford, MA). The DM11 dehalogenase was expressed and purified as previously described (*15*).

Steady-State Kinetics of Formaldehyde Formation. The kinetic parameters of DM11 were determined by a coupled assay with formaldehyde dehydrogenase from *P. putida.* Reactions were followed with a Perkin-Elmer Lambda 18 spectrophotometer at 25 °C in 1-mL gastight cuvettes. For each reaction, 10 nM DM11 was preincubated with 1 mM GSH, 1 unit (0.23 mg) of formaldehyde dehydrogenase from *P. putida* and 1 mM NAD in 100 mM potassium phosphate buffer (pH 8.0). The reaction was initiated by adding the substrate dihalomethane. The concentrations of substrates were varied between 0.8 μM and 1 mM for CH_2Cl_2, CH_2BrCl, CH_2Br_2, CH_2ClF, and CH_2ClI and 1.2 μM and 0.4 mM for CH_2I_2. The rate of production of formaldehyde was determined using linear regression to fit the initial rate of NADH production measured as an increase of absorbance at 340 nm. All measurements were done in triplicate and averaged. Data were fit to the Michaelis−Menten equation.

Kinetic parameters of DM11 with glutathione as the variable substrate were determined from the coupled assay carried out at constant concentration of substrate CH_2Cl_2 (1 mM), while the concentration of glutathione was varied between 25 μM and 10 mM. Data were fit to eq 1 to accommodate the substrate inhibition to obtain k_{cat}, K_M, and K_i.

$$V = \frac{k_{cat}[S][E]}{K_m + [S]\dfrac{[S]^2}{K_i}} \quad (1)$$

Iodide Release Assay. Enzyme activity for the iodine-containing substrates CH_2I_2, CH_2ClI, and CH_3CH_2I was also followed by iodide anion release spectrophotometrically at 226 nm. Iodide ion has a $\epsilon_{226} = 13\,000$ M^{-1} cm^{-1}). The experimentally determined $\Delta\epsilon$ values for each substrate were 15 200 M^{-1} cm^{-1} for CH_2I_2, 10 200 M^{-1} cm^{-1} for CH_2ClI, and 5500 M^{-1} cm^{-1} CH_3CH_2I. For each reaction, 25 nM DM11 was preincubated with 1 mM GSH in 100 mM potassium phosphate buffer (pH 8.0) at 25 °C. The reaction was initiated by the addition of the iodoalkane. Measurements were done on a Perkin-Elmer Lambda 18 spectrophotometer in a 1-mL gastight quartz cuvette. The rate of product formation was calculated by linear regression to fit the initial rate of iodide release. Data were fit to the Michaelis−Menten equation.

Pre-Steady-State Binding of Glutathione. Pre-steady-state kinetic data for glutathione binding were obtained with an Applied Photophysics Ltd. model SX17MV stopped-flow spectrometer at 25 °C with a 0.2-cm path-length cell. In the absorption mode, the wavelength was set at 239 nm to detect thiolate anion formation. In the fluorescence mode, the excitation was set at 295 nm and the intrinsic protein fluorescence observed through a 320-nm cutoff filter. Reactions contained 20 μM enzyme for the absorption measurements and 2 μM enzyme for the fluorescence measurements (concentrations observed in the cell). Solutions of enzyme and glutathione were made in 100 mM potassium phosphate buffer (pH 8.0). In general, 5−7 traces were averaged for each concentration of glutathione and fit to a single-exponential equation.

The dissociation rate of the GS^- from the enzyme complex was determined in a complementary experiment in which a solution of 40 μM enzyme containing 2 mM GSH was rapidly mixed with a solution of 40 mM GSO_3^-. The exponential decay of the A_{239} was followed to obtain the apparent off-rate of the thiolate.

Steady-State Fluorescence Titrations. Dissociation constants for the complex of DM11 with glutathione, glutathione sulfonate, or *S*-(ethyl)glutathione were determined by fluorescence titration. Steady-state fluorescence measurements were made on a SPEX Fluorolog-3 spectrofluorimeter (Jobin Yvon Horiba, Edison, NJ) in the constant-wavelength mode. The samples were excited at 295 nm, and the emission of samples at 340 nm was collected over 60 s. All measurements were done in triplicate and averaged. The decrease of fluorescence intensity of 0.6 μM of protein in 20 mM potassium phosphate buffer pH 8.0 was measured upon addition of the solution of GSH or its derivatives to a final concentration of 0.1−10 mM. Data were analyzed using eq 2

$$F = F_{max} - \frac{(F_{max} - F_s)[S]^n}{K_{0.5} + [S]^n} \quad (2)$$

where F = steady-state fluorescence emission, $F_{max} = F$ in the absence of substrate, F_s = protein fluorescence at saturating concentration of substrate, $K_{0.5}$ = dissociation constant, n = Hill coefficient.

Steady-State Kinetics of the Reaction with CH_3CH_2Br and CH_3CH_2Cl. The steady-state kinetics of DM11-catalyzed addition of GSH to bromoethane was initiated by addition of bromoethane (32 μM to 4 mM) in 100 mM HEPES (pH 8.0) to a solution of 1 μM DM11 and 1 mM GSH in the same buffer at 25 °C. The reaction was quenched by addition of 1 N HCl, neutralized with 1 N NaOH, derivatized with AQC, and analyzed by HPLC as described for the rapid-quench experiments below. Data were fit to the Michaelis−Menten equation.

Rapid-Quench Analysis of the Reaction of the DM11-Catalyzed Reaction of GSH and CH_3CH_2Br. Rapid-quench experiments were performed on a model RQF-3 Chemical-Quench-Flow apparatus (KinTek Corp., Austin, TX). The reactions were initiated by rapid mixing of a solution containing 60 or 100 μM DM11, 1.0 mM GSH, and 50 μM valine (as an internal standard for the following analysis) in 100 mM HEPES (pH 8.0) with the solution of 20 mM bromoethane and 50 μM valine in the same buffer. Reactions were also done at two higher concentrations with solutions containing 400 and 600 μM DM11 and 2 mM GSH, 50 μM valine. All reactions were quenched with 0.1 N HCl at various times from 10 ms to 100 s, and then each reaction mixture was neutralized with 1 N NaOH. For further analysis, the reaction mixtures were treated with 6-aminoquinolyl-*N*-hydroxysuccinimidyl carbamate (AQC) derivatizing agent. For derivatization, 10 μL of each reaction mixture was combined with 80 μL of borate buffer (supplied with the AQC reagent) and 10 μL of AQC solution, heated at 55 °C for 10 min, and analyzed by HPLC using a 4.6 mm × 25 cm Beckman C-18 Ultrasphere column. Samples (5 μL) were injected onto the column equilibrated with buffer containing 140 mM sodium acetate, 12.5 mM triethylamine, (pH 4.96). A gradient of acetonitrile (15−25%) was used to elute the reaction components over 20 min at a flow rate 1 mL/min. The data were fit into the eq 3 for two-step kinetic process that includes an initial burst followed by a steady-state reaction where A = burst amplitude, t = time, k_b = rate constant for the burst, and k_{cat} = steady-state turnover number.

$$y = A(1 - e^{-kbt}) + [E]k_{cat}t \quad (3)$$

Stopped-Flow Analysis of the DM11-Catalyzed Reaction of GSH and CH_3CH_2I. The DM11-catalyzed reaction of GSH and CH_3CH_2I was monitored at 25 °C with an Applied Photophysics Ltd. model SX17MV stopped-flow spectrometer at 25 °C with a 0.2-cm path-length cell. The reaction was initiated by rapidly mixing a solution of 40 μM DM11 containing 1.0 mM GSH in 100 mM potassium phosphate buffer (pH 8.0) with a solution of 5 mM CH_3CH_2I in the same buffer. To eliminate mixing artifacts, a difference trace was generated by subtraction of the absorbance data obtained from rapid mixing of 40 μM DM11 containing 1.0 mM GSH with buffer alone.

Effect of Viscosity on k_{cat}. The dependence of the steady-state kinetic parameters on the relative solution viscosity was determined by studying the DM11-catalyzed reactions with iodoalkanes or bromoethane in the presence of viscogens. The microviscosity of the solvent was varied by the addition of sucrose or glycerol to the reaction buffer. The relative viscosity of the buffers ranged from 1 to 2.35 for sucrose solutions and from 1 to 3.15 for glycerol-containing buffers. The relative viscosities of the solutions were measured in an Ostwald viscometer at 25 °C. The reactions were carried out as described above. Product formation was detected as an increase in the absorbance at 226 nm for the reaction with iodoalkanes or analyzed by HPLC for bromoethane after the derivatization with AQC.

Solvolysis of CH_3SCH_2Cl. Solvolysis of the intermediate analogue chloromethyl methyl sulfide in various mixtures of aqueous 1,4-dioxane was investigated by an asymmetric mixing stopped-flow spectrometry. The reaction was initiated by rapid mixing of 1 mM solution of chloromethyl methyl sulfide in dry 1,4-dioxane with 25 mM HEPES buffer (pH 8.0) at 1:1, 1:2.5, 1:5, and 1:10 (v/v) ratios of dioxane/water. The reaction was monitored in the UV at 4-nm intervals between 220 and 260 nm until the reaction was completed. The rates of solvolysis of chloromethyl methyl sulfide were calculated from the evolution of the UV spectra with the Pro-Kineticist global analysis software and plotted against the concentration of water in the final mixture.

RESULTS

Steady-State Kinetics of the DM11-Catalyzed Reactions with Dihalomethanes. The steady-state kinetic analysis of reactions with six dihalomethane substrates summarized in Table 1 shows essentially the same trends in k_{cat} and k_{cat}/K_M previously observed under different experimental conditions (*15*). The turnover numbers are remarkably similar with the exception of CH_2ClF, which is known to form a relatively stable GS-CH_2F intermediate on the way to formaldehyde (*3*). If the chemical decomposition of GS-CH_2F is the rate-limiting step in formaldehyde formation, then the observed turnover number of 0.009 s^{-1} suggests a $t_{1/2} \approx 77$ s for the

Table 1: Steady-State Kinetic Parameters of DM11 toward Dihalomethane Substrates by the Coupled Assay with Formaldehyde Dehydrogenase or by Iodide Ion Release

substrate	k_{cat} (s^{-1})	k_{cat}/K_M (M^{-1} s^{-1})	K_M (μM)
CH_2Cl_2	1.51 ± 0.06	$(4.9 \pm 1.0) \times 10^4$	31 ± 6
CH_2Br_2	3.18 ± 0.08	$(1.0 \pm 0.2) \times 10^6$	3.1 ± 0.5
CH_2BrCl	1.00 ± 0.01	$(6.25 \pm 0.07) \times 10^5$	1.62 ± 0.01
CH_2ClF	0.009 ± 0.001	$(1.7 \pm 0.6) \times 10^2$	53 ± 18
CH_2ClI	1.03 ± 0.02 (1.4 ± 0.1)[a]	$(5.4 \pm 0.9) \times 10^5$	2.0 ± 0.3
CH_2I_2	1.31 ± 0.05 (1.5 ± 0.1)[a]	$(7.7 \pm 1.7) \times 10^5$	1.7 ± 0.4

[a] Values of k_{cat} in parentheses are based on iodide release determined spectrophotometrically.

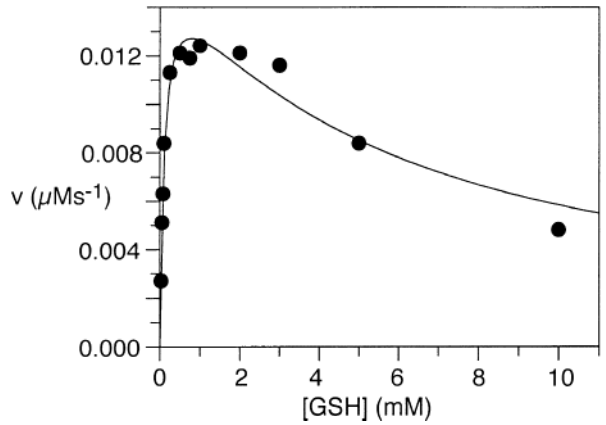

FIGURE 1: Dependence of the initial velocity of formaldehyde formation on the concentration of GSH. The line is a fit to the expression for saturation kinetics with substrate inhibition (eq 1) with $k_{cat} = 1.50 \pm 0.08$ s^{-1}, $K_M = 99 \pm 14$ μM and $K_i = 7.3 \pm 1.5$ mM.

intermediate. This is consistent with previous suggestions that the solvolysis of GS-CH_2F occurs on the time scale of minutes (*3*).

In contrast to k_{cat}, the values for k_{cat}/K_M, which reflect the activation barrier(s) between the free enzyme and substrate and the first irreversible step, vary somewhat more and correlate reasonably well with the expected electrophilicity of the methyl carbon and the leaving group ability of the first departing halide. The coupled formaldehyde dehydrogenase assay detects the formation of formaldehyde, which is at least two steps removed from the initial displacement reaction. However, the spectrophotometric detection of iodide ion in reactions of CH_2ClI and CH_2I_2 looks at steps preceding formaldehyde formation. The turnover numbers for these two substrates in both assays are similar and indicate that the reaction is behaving as expected for a steady-state enzymatic reaction.

The steady-state kinetics toward CH_2Cl_2 with GSH as the variable substrate is shown in Figure 1. The kinetic parameters are consistent with those reported previously (*3*, *9*, *13*, *14*), but the positive cooperativity with GSH reported in other work under different experimental conditions (*9*, *10*, *13*) was not observed. In contrast, a marked substrate inhibition by GSH is observed at concentrations >2 mM (Figure 1). Similar behavior has been previously noted (*3*). All steady-state kinetic assays were therefore conducted at [GSH] < 2 mM.

Interaction of the Enzyme with GSH. The interaction of GSH with the enzyme was investigated by steady-state fluorescence titration and by stopped-flow kinetics of the

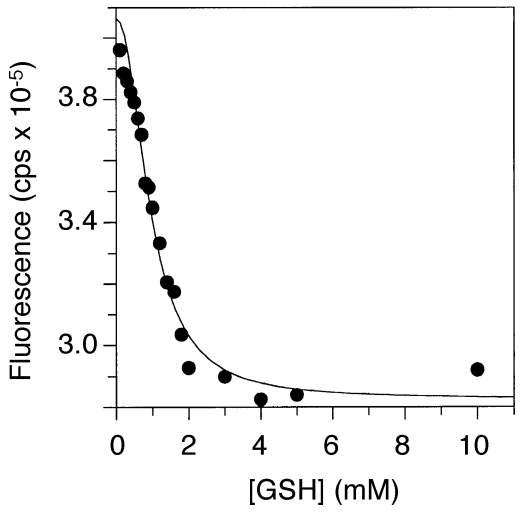

FIGURE 2: Fluorescence titration of 0.6 μM DM11 enzyme with GSH at pH 8.0 and 25 °C. The samples were excited at 295 nm, and the emission was monitored at 340 nm with an integration time of 60 s. The line is a regression fit of the data to eq 2 with the $K_{0.5}$ and n values reported in the text.

approach to equilibrium. Titration of the enzyme with GSH results in a 30% decrease in the intrinsic protein fluorescence. The binding isotherm suggests that the interaction of GSH with the dimeric enzyme exhibits positive cooperativity as illustrated in Figure 2 with a $K_{0.5} = 0.88 \pm 0.07$ mM and $n = 2.1 \pm 0.2$. The binding of the analogue glutathione sulfonate (GSO_3^-) is similar with $K_{0.5} = 1.26 \pm 0.06$ mM and $n = 2.3 \pm 0.1$.

The kinetics of the approach to equilibrium for the binding of GSH to DM11 appears to occur as a two-step process. The binding of GSH is accompanied by slow thiolate formation as indicated in Figure 3A. The observed rate constant for thiolate formation varies as a linear function [GSH] (Figure 3C) in the concentration range that can be studied (≤10 mM due to high background absorbance at 239 nm). The apparent off-rate of the thiolate is too small (< 0.1 s^{-1}) to be accurately measured in this experiment. Interestingly, the maximum amplitude of the thiolate signal indicates a $\Delta\epsilon_{239} \approx 2000$ M^{-1} cm^{-1}/active site, which is about half that expected based on the known $\epsilon_{239} = 5000$ M^{-1} cm^{-1} for GS^- (*16*).

The changes in fluorescence on GSH binding to the enzyme occur on the same time scale as thiolate formation (Figure 3B). However, in this instance, the concentration dependence of the kinetics can be evaluated at much higher [GSH] where saturation behavior is observed. The hyperbolic dependence of k_{obs} on [GSH] is consistent with a mechanism such as that in Scheme 3 in which the slow ionization of enzyme-bound GSH is preceded by a rapid equilibrium binding of the peptide where the dissociation constant for the first step, $K_s = k_{-1}/k_1$. The dependence of k_{obs} on [GSH] is given by eq 4.

$$k_{obs} = k_{-2} + k_2[GSH]/(K_s + [GSH]) \quad (4)$$

$$k_{obs} \approx k_{-2} + k_2[GSH]/K_s \quad (5)$$

The fluorescence data indicate that $K_s = 130 \pm 30$ mM, $k_2 = 59 \pm 8$ s^{-1}, and $k_{-2} = 0.4 \pm 0.3$ s^{-1}. When $K_s \gg$ [GSH] as in the thiolate formation experiments, the dependence of

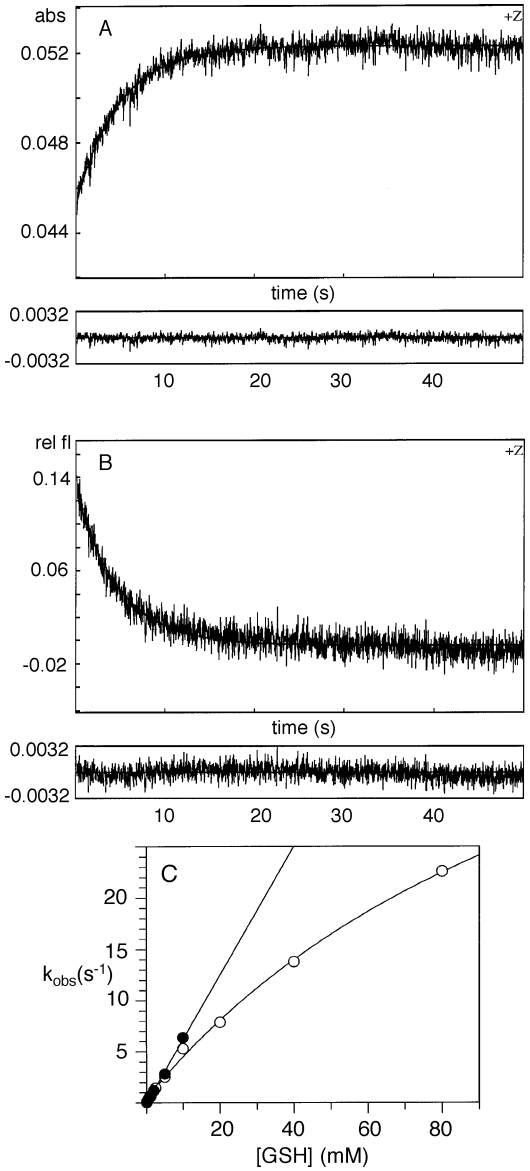

FIGURE 3: (A) Thiolate formation on rapid mixing of the enzyme with GSH at pH 8.0 and 25 °C. Absorbance was monitored at 239 nm in a 0.2-cm cell with [E] = 20 μM and [GSH] = 400 μM. The lower trace is the residual to a fit of the data to a single exponential with a $k_{obs} = 0.211 \pm 0.002$ s^{-1}. (B) Fluorescence change on rapid mixing of enzyme and GSH at pH 8.0 and 25 °C. The sample, [E] = 2 μM and [GSH] = 500 μM, was excited at 295 nm and total fluorescence was observed through a 320-nm cutoff filter. The lower trace is the residual to a fit of the data to a single exponential with a $k_{obs} = 0.208 \pm 0.003$ s^{-1}. (C) Dependence of k_{obs} on [GSH]. The data for thiolate formation (●) were fit to eq 5 with $k_2/K_s = 630 \pm 10$ M^{-1} s^{-1} and $k_{-2} \approx 0$. The data for the fluorescence change (○) were fit to eq 4 with $K_s = 130 \pm 30$ mM, $k_2 = 58 \pm 9$ s^{-1} and $k_{-2} = 0.4 \pm 0.3$ s^{-1}.

Scheme 3

$$E \underset{k_{-1}}{\overset{k_1[GSH]}{\rightleftharpoons}} E{\cdot}GSH \underset{k_{-2}}{\overset{k_2}{\rightleftharpoons}} E^*{\cdot}GS^-$$

k_{obs} on [GSH] reduces to eq 5. Thus, $k_2/K_s = 630 \pm 10$ M^{-1} s^{-1} for thiolate formation is in reasonable agreement with that calculated from the fluorescence kinetics of 450 ± 90 M^{-1} s^{-1}. Unlike the steady-state fluorescence titration, there is no evidence of positive cooperativity in the stopped-flow kinetics.

Table 2: Steady State Kinetic Parameters of DM11 toward Monohaloethane Substrates by HPLC Assay or by Iodide Ion Release

substrate	k_{cat} (s^{-1})	k_{cat}/K_M (M^{-1} s^{-1})	K_M (μM)
CH_3CH_2Cl	0.10 ± 0.01	(3.0 ± 0.2) × 10^2	330 ± 46
CH_3CH_2Br	0.14 ± 0.01	(4.2 ± 0.2) × 10^2	330 ± 40
CH_3CH_2I[a]	0.15 ± 0.01	(3.8 ± 0.07) × 10^4	39 ± 7

[a] Values are based on iodide release determined spectrophotometrically.

The net k_{-2} for the conformational transition and thiolate formation in the complex was estimated to be < 0.1 s^{-1} and therefore too small to be accurately measured in the approach to equilibrium kinetics. It is possible to measure the rate constant for this transition by preforming the E*·GS$^-$ complex and then trapping the free enzyme with a high concentration of the substrate analogue GSO_3^- in the stopped flow (*17*−*19*). Rapid mixing of E*·GS$^-$ ([E] = 20 μM, [GSH] = 1 mM final concentration) with GSO_3^- (20 mM final concentration) results in the exponential decay of the thiolate absorbance at 239 nm with a $k_{-2} = 0.0147 \pm 0.0004$ s^{-1}. With the values of K_s, k_2, and k_{-2} in hand an overall equilibrium constant ($K_D^{GS^-}$) for thiolate formation on the enzyme of 30 μM can be calculated.

Kinetics of Addition of GSH to Monohaloethanes. To examine the initial displacement step in isolation, the reactions with CH_3CH_2Cl, CH_3CH_2Br, and CH_3CH_2I were investigated. These molecules are reasonable steric analogues of dihalomethanes given that a methyl group approximates the size of a halogen. The steady-state kinetic parameters for these substrates are presented in Table 2. Again, the values of k_{cat} for these substrates are essentially identical, indicating a common rate-limiting step in turnover. In contrast, the values of k_{cat}/K_M reflect the relative leaving group ability of the halides.

Inasmuch as the peptide products of these reactions are the same, the most reasonable kinetic scenario is that release of GSEt is the rate-limiting step in turnover of the enzyme. If this were true, then a burst of GSEt would be expected before the enzyme entered the steady-state. Figure 4 illustrates the results of rapid-quench experiments with CH_3CH_2Br as the substrate. The steady-state turnover, which has a k_{cat} that is close to that observed in steady-state kinetic experiments, is clearly preceded by a burst of product that is equivalent to about half of the concentration of active sites. The two surprising results of these experiments are the amplitude of the burst phase and the magnitude of the rate constant for the burst estimated to be between 50 and 150 s^{-1}. Clearly, the first chemical step of the reaction is much faster than the subsequent kinetic event(s) that limits turnover. The amplitude of the burst, *A*, was measured at four enzyme and two GSH concentrations and, within the error of the experiments, did not vary from half the concentration of the active sites as indicated in Table 3. These observations indicate that the dimeric enzyme functions with half-the-sites-reactivity.

In principle, it should also be possible follow the pre-steady-state formation of I$^-$ by stopped-flow spectroscopy at 226 nm. However, the spectral contribution of GS$^-$ and the high background absorbance of the reaction mixtures at wavelengths <230 nm make such experiments difficult to execute and interpret. Nevertheless, stopped-flow difference

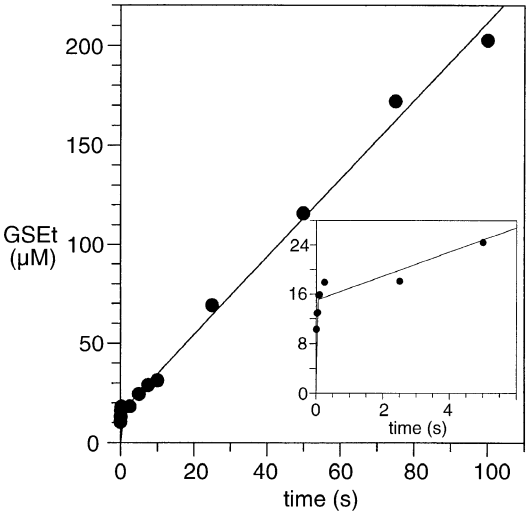

FIGURE 4: Burst kinetics of GSEt formation. A solution of enzyme and GSH in 100 mM HEPES buffer (pH 8.0) was rapidly mixed with buffer containing CH_3CH_2Br. The final reaction mixture contained 30 μM enzyme active sites, 0.5 mM GSH, and 10 mM CH_3CH_2Br. The reactions were quenched and the GSEt concentrations analyzed as described in Experimental Procedures. The data points are averages of three independent determinations. The solid line represents a fit of the data to the expression $[GSEt] = A(1 - e^{-kbt}) + [E]k_{cat}t$ with, $A = 15 \pm 1$ μM, $k_b = 96 \pm 56$ s^{-1}, and $k_{cat} = 0.13 \pm 0.01$ s^{-1}. The inset more clearly shows the burst phase of the reaction.

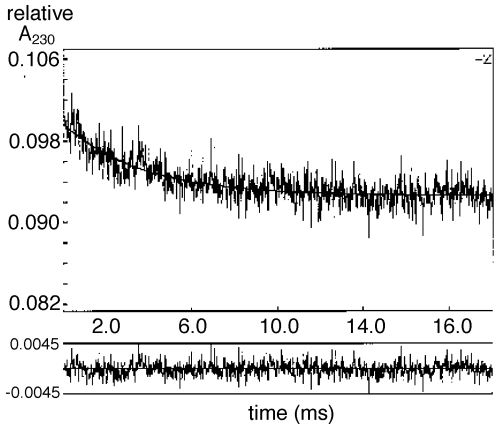

FIGURE 5: Difference stopped-flow kinetic trace of the reaction of 20 μM DM11 and 0.5 mM GSH with 2.5 mM CH_3CH_2I. The reaction was carried out at 25 °C (pH 8.0) by rapidly mixing a solution of 40 μM DM11, 1.0 mM GSH in 100 mM KH_2PO_4 buffer (pH 8.0). The difference trace was generated by subtraction of the absorbance data obtained from rapid mixing 40 μM DM11 containing 1.0 mM GSH with buffer alone. The resulting trace no longer contains the mixing artifacts observed at <2 ms. The bottom trace is the residual of a fit of the data to single-exponential expression with $k_{obs} = 270 \pm 10$ s^{-1}.

Table 3: Amplitude of the Burst of GSEt in the Pre-Steady-State Reaction of $E{\cdot}GS^-$ with CH_3CH_2Br as a Function of the Concentration of the Enzyme and GSH

[enzyme] (μM)	[GSH] (mM)	A/[E] [GSEt]/[E]
30	0.5	0.5 ± 0.1
50	0.5	0.6 ± 0.1
200	1.0	0.56 ± 0.05
300	1.0	0.53 ± 0.03

spectroscopy of the pre-steady-state reaction of CH_3CH_2I with a solution of $E{\cdot}GS^-$ clearly indicates a rapid decrease in the absorbance at 230 nm that occurs with a rate constant

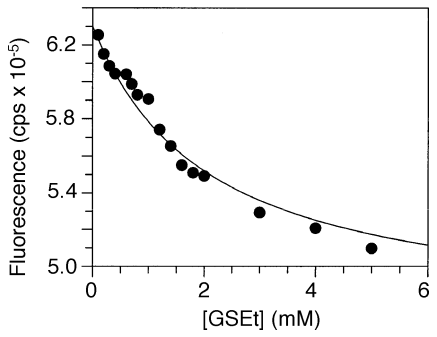

FIGURE 6: Fluorescence titration of 0.6 μM DM11 enzyme with GSEt at pH 8.0 and 25 °C. The samples were excited at 295 nm and the emission monitored at 340 nm with an integration time of 60 s.

of 270 ± 10 s^{-1} (Figure 5). It seems likely that this spectral change is associated with the chemical step of the reaction and that it reflects the combined loss of thiolate and increase in I^- on reaction of $E{\cdot}GS^-$ with CH_3CH_2I. The rate constant for this process is somewhat larger than that observed for the burst of GSEt in the reaction with CH_3CH_2Br and consistent with the expected higher chemical reactivity of CH_3CH_2I.

Binding of GSEt to the Enzyme. The kinetics of binding of GSEt to the enzyme was examined by stopped-flow spectroscopy and steady-state fluorescence titration. Steady-state fluorescence titration of the enzyme with GSEt indicates a hyperbolic binding isotherm with a dissociation constant of 2.1 ± 0.1 mM (Figure 6). This contrasts with the cooperative behavior observed in the binding of GSH and GSO_3^-.

The kinetics of the approach to equilibrium were determined as illustrated in Figure 7. The observed rate of binding is quite slow, and the dependence of k_{obs} on [GSEt] appears linear with an apparent second-order rate constant of 126 ± 2 M^{-1} s^{-1}. The fact that this rate is so far from the diffusion limit indicates that an isomerization of the protein occurs prior to or after the binding event. Most importantly, the apparent $k_{off} = 0.075 \pm 0.008$ s^{-1} is close to the observed turnover numbers (ca 0.10−15 s^{-1}) with CH_3CH_2Cl, CH_3CH_2Br, and CH_3CH_2I. This is a good indication that peptide product release is likely the rate-limiting step in turnover of these substrates.

Dependence of the Enzyme-Catalyzed Reactions on Viscosity. If a diffusive step such as product release controls the turnover of the enzyme, then k_{cat}^0 observed at a reference viscosity η^0 will be related to k_{cat} observed at some higher viscosity, η, in the presence of a viscogen by $k_{cat}^0/k_{cat} = \eta/\eta^0$. Thus, a plot of the inverse relative rate constant vs the relative viscosity (η/η^0) should be linear with a slope = 1 when the release of product is limited by a strictly diffusive barrier or have a slope = 0 if a nondiffusive barrier such as chemistry is rate-limiting. Figure 8 illustrates the dependence of k_{cat}^0/k_{cat} on relative viscosity for three different substrates and two different viscogens. The slopes of the plots range from 0.7 to 1.1 and are consistent with a rate-limiting diffusive step in the turnover of the enzyme.

Solvolysis of CH_3SCH_2Cl. The kinetics of solvolysis of chloromethyl methyl sulfide was investigated in a series of dioxane/water mixtures to provide an estimate of the solvolytic stability of the GS-CH_2Cl intermediate. The com-

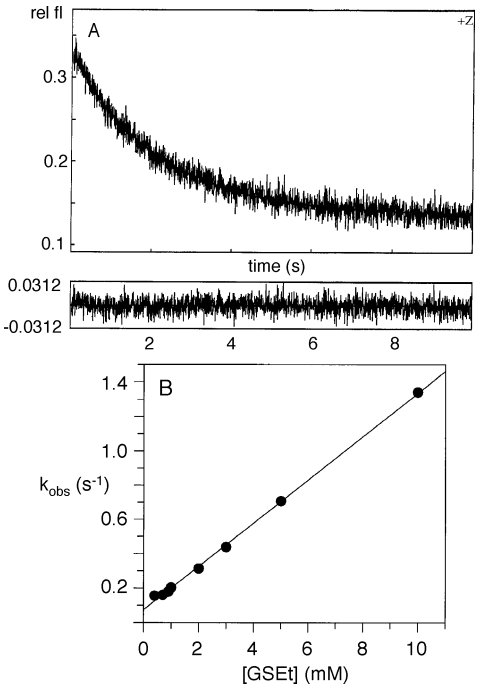

FIGURE 7: (A) Fluorescence change on rapid mixing of the DM11 enzyme with GSEt at pH 8.0 and 25 °C. The sample was excited at 295 nm and total fluorescence was observed through a 320 nm cutoff filter. (B) Dependence of k_{obs} for the fluorescence change on [GSEt]. The line is a least-squares fit of the data with a slope = 126 ± 2 M^{-1} s^{-1} and an intercept of 0.075 ± 0.008 s^{-1}.

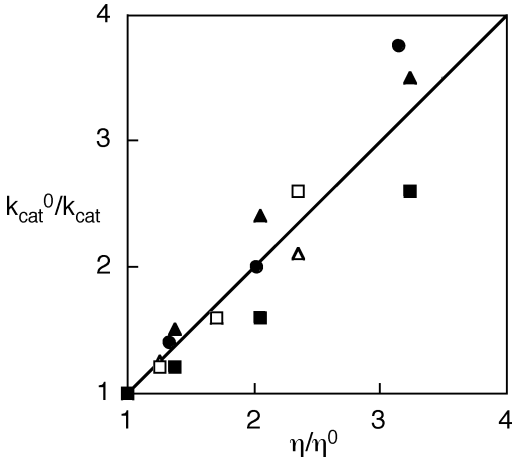

FIGURE 8: Dependence of k_{cat}^0/k_{cat} on the relative viscosity of the reaction medium. The experimental data points are (●) CH_3CH_2-Br in glycerol, slope = 1.11 ± 0.06; (▲) CH_3CH_2I in glycerol, slope = 1.12 ± 0.08; (Δ) CH_3CH_2I in sucrose, slope = 0.81 ± 0.02; (■) CH_2I_2 in glycerol, slope = 0.72 ± 0.05; (□) CH_2I_2 in sucrose, slope = 1.12 ± 0.1. The line illustrated has a slope of 1.

pound is very stable in anhydrous dioxane (*20*) but solvolyzes rapidly in the presence of water as illustrated in Figure 8. The observed rate constant for solvolysis ranges from of 1.1 s^{-1} ($t_{1/2}$ = 0.63 s) in 1:1 dioxane/water to 64 s^{-1} ($t_{1/2}$ = 11 ms) in 1:10 dioxane/water. The solvolysis occurs on a time scale that is at least as fast as enzyme turnover. The nonlinear dependence of the rate constant for solvolysis on [H_2O] is expected since the reaction proceeds through the cationic intermediate, $GS^+{=}CH_2$, which is stabilized by the higher dielectric constant of solvent mixtures with increasing concentrations of water.

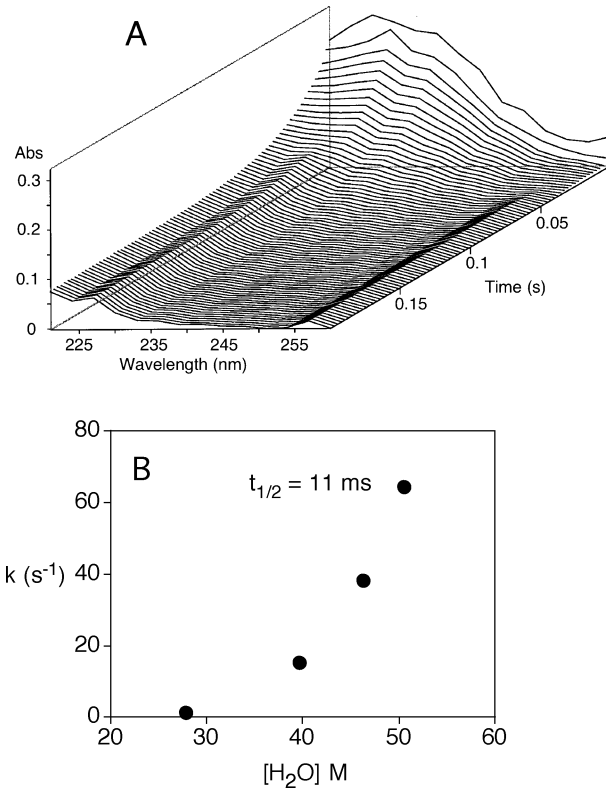

FIGURE 9: (A) Three-dimensional plot of the evolution of the UV spectrum during the hydrolysis of CH_3SCH_2Cl after rapid asymmetric mixing (1:5) of CH_3SCH_2Cl in dioxane with 25 mM HEPES (pH 8.0). Kinetic traces were acquired at 4-nm intervals between 260 and 220 nm and processed with Pro-Kineticist program. The evolution of the spectra was fit to a single exponential with a rate constant of 38.2 s^{-1}. (B) Dependence of the observed rate constant on the concentration of water.

DISCUSSION

Interaction of the Enzyme with GSH. The interaction of the DM11 enzyme with GSH and related molecules appears to involve at least two species. Although positive cooperativity is observed in the binding of GSH in equilibrium experiments, it is not apparent in the approach to equilibrium kinetics or in the steady-state kinetics. It is interesting to note that cooperativity in the equilibrium titrations is only observed in the binding of GS^- and GSO_3^-, molecules that provide a negative charge near the sulfur. The substrate inhibition by GSH indicates that there is a second GSH binding site. Whether this phenomenon is related to occupancy of the second subunit in the dimer is not clear.

The rather slow spectral changes observed in the approach to equilibrium experiments are indicative of a two-step process involving a rapid preequilibrium binding of the peptide that is followed by a slow conformational transition associated with formation of a tightly bound thiolate complex. This behavior is very similar to that previously reported for the microsomal enzyme, MGST1 (*17*). The lack of evidence for positive cooperativity in the approach equilibrium kinetics suggests that the equilibrium binding and kinetic experiments are looking at different phenomena. There is, for example, a large discrepancy in the apparent dissociation constants of GSH ($K_d^{GS^-}$ = 30 μM vs $K_{0.5}$ = 1.8 mM) obtained from the two experiments. The principal differences between the two types of experiments are the

Scheme 4

$$E \underset{K_s = 0.13\ M}{\overset{GSH}{\rightleftharpoons}} E{\cdot}GSH \underset{0.015\ s^{-1}}{\overset{60\ s^{-1}}{\rightleftharpoons}} E^{*}{\cdot}GS^{-} \rightleftharpoons HSG{\cdot}E^{*}{\cdot}GS^{-}$$

concentrations of the enzyme and the time scale, with the equilibrium experiments being at lower protein concentration and on a much longer time scale. It could be that the cooperative behavior is manifest primarily in the off-rates of GS^-, which does not contribute significantly to the approach to equilibrium kinetics.

Half-the-Sites-Reactivity. Several pieces of evidence suggest that the DM11 enzyme exhibits half-the-sites-reactivity, an extreme example of negative cooperativity. First and foremost is the fact that the saturation of the enzyme with GSH at pH 8 results in one equivalent of thiolate per dimer. Second, the amplitude of the burst of product formation observed in the rapid-quench experiments corresponds to half that expected based on the concentration of active sites under conditions of [GSH] $\gg K_d^{GS^-}$. Finally, as mentioned above, the substrate inhibition observed at high [GSH] is consistent with a nonproductive occupancy of the second GSH site in the dimer. Taken together, these observations suggest that the two GSH binding sites in the dimer do not behave independently.

One possible mechanism for the interactions is given in Scheme 4 where the complex with the highest catalytic activity is $E^*{\cdot}GS^-$. The fully loaded complex $HSG{\cdot}E^*{\cdot}GS^-$ may be less active, but once the thiolate reacts with a haloalkane or product departs the second site is free to form thiolate.

Rate-Limiting Step(s) in Catalysis. All of the experimental evidence presented in this paper suggests that product release is a major contributor to the rate-limiting step in catalysis. The more difficult question to answer, particularly with dihalomethane substrates, is the identity of the product whose release is rate limiting. The issue is much easier to address with the monohaloethane substrate analogues. The observed burst of GSEt product can be accommodated by mechanisms involving either rate-limiting release of GSEt or halide. The latter possibility seems unlikely since there is no difference in the observed turnover numbers as the identity of the leaving group (halide) is changed.

The chemistry after the initial displacement reaction considerably complicates the analysis with dihalomethane substrates. Again, it is likely that product release is the rate-limiting step. However, as illustrated in Scheme 2, the product that is released in the slow step could be one of several species, $GS\text{-}CH_2X$, $GS\text{-}CH_2OH$, halide, or even formaldehyde. The latter possibility (the lower pathway in Scheme 2) is an interesting one in which the peptide remains bound to the enzyme during hydrolysis of the intermediates and release of formaldehyde. This mechanism is difficult to assess since the rates of hydrolysis of the $GS\text{-}CH_2X$ and $GS\text{-}CH_2OH$ on the enzyme surface are not known. This mechanism would predict similar turnover numbers for all of the substrates with the exception of CH_2ClF, which forms a relatively stable intermediate. Alternatively, if halide release were rate limiting, then there should be some correlation between the first departing halide and the turnover number. This does not seem to be the case.

The rapid rate of solvolysis of CH_3SCH_2Cl in mixed aqueous−organic solvents suggests that perhaps solvolysis of $E{\cdot}GS\text{-}CH_2X$ (where X = Cl, Br, or I) may occur more rapidly or at least on the same time-scale as peptide product release. The kinetics of solvolysis on the enzyme surface obviously depends on the structure and solvent accessibility of the active site, which at this point are not known. It is worth noting that the solvolysis of CH_3SCH_2Cl in 50% dioxane/water occurs with a rate constant of about 1 s^{-1}, which is comparable to the turnover number of the enzyme.

Peptide dissociation from the enzyme, in the two instances where it has been measured, is slow, with rate constants between 0.015 s^{-1} (GS^-) and 0.075−0.14 s^{-1} (GSEt). From this and the above observations, a good case can be made that the release of the peptide product is sufficiently slow to permit hydrolysis of the $GS\text{-}CH_2X$ intermediate while still bound to the enzyme. The dissociating species and kinetic contributors to turnover in this scenario are $GS\text{-}CH_2OH$ or $CH_2(OH)_2$. In fact, the results with monohaloethane substrates indicate that peptide product release may be as much as an order of magnitude slower than the turnover numbers observed with dihalomethane substrates. Therefore, it seems probable that $CH_2(OH)_2$ is the principal dissociating species so that individual enzyme-bound GS^- molecules undergo multiple turnovers before being released from the active site (Scheme 2). The small differences in the turnover numbers with the different dihalomethane substrates may be due to kinetic contributions of other species in Scheme 2.

Biological Consequences of the Mechanism. The biological consequences of slow product release from the DM11 enzyme would be a decrease in the genotoxicity of dichloromethane catabolism in microorganisms. The mechanism may be entirely passive and need not involve additional catalytic chemistry to decompose the intermediate. Retaining the peptide product in the active site for sufficient time to allow the highly reactive $GS\text{-}CH_2Cl$ to hydrolyze decreases the probability that it will react with cellular macromolecules such as DNA. Clearly, this would be a selective advantage for a microorganism feeding on dihalomethanes.

ACKNOWLEDGMENT

We thank Hong Zang for assisting in the rapid quench experiments and Fred Guengerich for many helpful discussions.

REFERENCES

1. Thier, R., Taylor, J. B., Pemble, S. W., Humphreys, W. G., Persmark, M, Ketterer, B., and Guengerich, F. P. (1993) *Proc. Natl. Acad. Sci. U.S.A. 90*, 8576−8580.
2. Hashmi, M., Dechert, S., Dekant, W., and Anders, M. W. (1994) *Chem. Res. Toxicol. 7*, 291−296.
3. Blocki, F. A., Logan, M. S. P., Baoli, C., and Wackett, L. P. (1994) *J. Biol. Chem. 269*, 8826−8830.
4. Graves, R. J., Callander, R. D., and Green, T. (1994) *Mutat. Res. 320*, 235−243.
5. Thier, R., Muller, M., Taylor, J. B., Pemble, S. E., Ketterer, B., and Guengerich, F. P. (1995) *Chem. Res. Toxicol. 8*, 465−472.
6. Their, R., Pemble, S. E., Kramer, H., Taylor, J. B., Guengerich, F. P., and Ketterer, B. (1996) *Carcinogenesis 17*, 163−166.
7. Oda, Y., Yamazaki, H., Their, R., Ketterer, B. Guengerich, F. P., and Shimada, T. (1996) *Carcinogenesis 17*, 297−302.

8. Shimada, T., Yamazaki, H., Oda, Y., Hiratsuka, A., Watabe, T., and Guengerich, F. P. (1996) *Chem. Res. Toxicol. 9*, 333−340.
9. Scholtz, R., Wackett, L. P., Egli, C., Cook, A. M., and Leisinger, T. (1988) *J. Bacteriol. 170*, 5698−5704.
10. Vuilleumier, S., and Leisinger, T. (1996) *Eur. J. Biochem. 239*, 410−417.
11. Vuilleumier, S. (1997) *J. Bacteriol. 179*, 1431−1441.
12. Vuilleumier, S. and Pagni, M. (2002) *Appl. Microbiol. Biotechnol. 58*, 138−146.
13. Gisi, D., Leisinger, T., and Vuilleumier, S. (1999) *Arch. Toxicol. 73*, 71−79.
14. Wheeler, J. B., Stourman, N. V., Thier, R., Dommermuth, A., Vuilleumier, S., Rose, J. A., Armstrong, R. N., and Guengerich, F. P. (2001) *Chem. Res. Toxicol. 14*, 1118−1127.
15. Wheeler, J. B., Stourman, N. V., Armstrong, R. N., and Guengerich, F. P. (2001) *Chem. Res. Toxicol. 14*, 1107−1117.
16. Graminski, G. F., Kubo, Y., and Armstrong, R. N. (1989) *Biochemistry 28*, 3562−3568.
17. Morgenstern, R., Svensson, R., Bernat, B. A., and Armstrong, R. N. (2001) *Biochemistry 40*, 3378−3384.
18. Johnson, W. W., Liu, S., Ji, X., Gilliland, G. L., and Armstrong, R. N. (1993) *J. Biol. Chem. 268*, 11508−11511.
19. Parsons, J. F., Xiao, G., Gilliland, G. L., and Armstrong, R. N. (1998) *Biochemistry 37*, 6286−6294.
20. Bohme, V. H., Fischer, H., and Frank, R. (1949) *Ann. 563*, 54−72.

BI035016R